J Stat Phys (2017) 166:1209–1225
DOI 10.1007/s10955-017-1718-x

Noisy Hegselmann-Krause Systems: Phase Transition and the $2R$-Conjecture

Chu Wang[1,2] · Qianxiao Li[1] · Weinan E[3] · Bernard Chazelle[4]

Received: 6 August 2016 / Accepted: 11 January 2017 / Published online: 27 January 2017

Abstract The classic Hegselmann-Krause (HK) model for opinion dynamics consists of a set of agents on the real line, each one instructed to move, at every time step, to the mass center of the agents within a fixed distance R. In this work, we investigate the effects of noise in the continuous-time version of the model as described by its mean-field Fokker-Planck equation. In the presence of a finite number of agents, the system exhibits a phase transition from order to disorder as the noise increases. We introduce an order parameter to track the phase transition and resolve the corresponding phase diagram. The system undergoes a phase transition for small R but none for larger R. Based on the stability analysis of the mean-field equation, we derive the existence of a forbidden zone for the disordered phase to emerge. We also provide a theoretical explanation for the well-known $2R$ conjecture, which states that, for a random initial distribution in a fixed interval, the final configuration consists of clusters separated by a distance of roughly $2R$. Our theoretical analysis confirms previous simulations and predicts properties of the noisy HK model in higher dimension.

Keywords Collective behavior · Opinion dynamics · Cluster formation · Phase transition · Dynamic networks

✉ Chu Wang
chuw@math.princeton.edu; chuwang.math@gmail.com

Qianxiao Li
qianxiao@math.princeton.edu

Weinan E
weinan@math.princeton.edu

Bernard Chazelle
chazelle@cs.princeton.edu

1 The Program in Applied and Computational Mathematics, Princeton University, Princeton, NJ 08540, USA

2 Nokia Bell Labs, 600 Mountain Avenue, Murray Hill, NJ 07974, USA

3 Department of Mathematics and the Program in Applied and Computational Mathematics, Princeton University, Princeton, NJ 08540, USA

4 Department of Computer Science, Princeton University, Princeton, NJ 08540, USA

1 Introduction

Network-based dynamical systems have received a surge of attention lately. In these systems, typically, a set of agents will interact by communicating through a dynamic graph that evolves endogenously. The popularity of the model derives from its widespread use in the life and social sciences [1,4,5,7,8,12,18]. Much of the difficulty in analyzing these systems stems from the coupling between agent dynamics and evolving graph topology [8]. If the system is diffusive and the information transfer between agents is symmetric, it usually converges to an attractor under mild assumptions [6,26]. In the absence of symmetry, however, the system can exhibit the whole range of dynamical regimes, from periodicity to chaos [8].

The Hegselmann-Krause (*HK*) model is the classic representative of the diffusive type. It consists of a fixed number N of agents, each one located at $x_k(t)$ on the real line. At each time step, every agent moves to the mass center of all the others within a fixed distance R. The position of an agent represents its "opinion". The underlying assumption is that people are immune to the influence of others whose opinions greatly differ from their own. In particular, two groups of agents initially separated by a distance of R or more will form decoupled dynamical systems with no interaction between them. *HK* systems are known to converge in finite time, but the relationship between the initial and final profiles remains mysterious. The celebrated $2R$ *conjecture* states, for a random initial distribution in a fixed interval, the final configuration consists of clusters separated by a distance of roughly $2R$ [3].

It is useful to enlarge the model by introducing noise into the dynamics [29]. Stochasticity can be invoked to capture nonobservable factors operating at smaller scales. Analytically, it has the benefits of nudging the system away from pathological configurations. By tuning the noise level as we would the temperature of a thermodynamical system, we can vary the dynamics from chaos to fixed-point attraction and uncover phase transitions in the process. To simplify the analysis, we model the system with a stochastic differential equation (SDE) for the continuous-time version of the *HK* model and focus on its mean-field approximation in the form of a Fokker-Planck type partial differential equation (PDE) governing the agent density evolution. This formulation of noisy *HK* systems in the thermodynamic limit can be derived from first principles and seems well-supported by computer simulation.

We review related works in Section 2 and formally introduce the model in Section 3. In Section 4, we propose an order parameter to describe and analyze the system dynamics, along with the investigation of the system bistability and the phase diagram. We find that the system undergoes a phase transition for small R but none for larger R. Based on the stability analysis of the mean-field equation (Section 6), we derive the existence of a forbidden zone for the disordered phase to emerge. This puts us in a position, building on previous work, to provide a theoretical explanation for the 2R conjecture in the thermodynamic limit. Our theoretical analysis confirms previous simulations and predicts properties of the noisy *HK* model in higher dimension. In Section 7, we discuss the origin of different phase behaviors in the SDE model and the PDE model.

2 Prior Work

The convergence of the classical *HK* system was established in a number of articles [16,21,26] and subsequent work provided increasingly tighter bounds on the convergence rate, with a current bound of $O(N^3)$ [2,25]. While there exists a worst-case lower bound of $\Omega(N^2)$ [31], computer simulations suggest that, in general, the convergence rate is much faster. The model

extends naturally to higher dimension by interpreting R as the Euclidean distance. Polynomial upper bounds are known for that case as well [6], with the current best being $O(N^4)$ [24]. We note that the convergence time can be significantly lowered if certain "strategic" agents are allowed to move anywhere at each step [20]. For general consensus and stability properties of the infinite-horizon profile, we refer the interested reader to [14,22,23,30].

Attempts to analyze natural extensions of the *HK* model to the nonsymmetric case have proven surprisingly frustrating. While it is known that diffusive influence systems (the generalization of *HK* model) can have limit cycles and even chaotic behaviors, the simple fact of allowing each agent to pick its own interval produces dynamics that remains unresolved to this day. Numerical simulations suggest that such systems converge but a proof has been elusive. All we know is that if each agent can pick its interval freely in $\{0, R\}$, the system still converges [10]; in other words, taking the original *HK* system and fixing some of the agents once does not change the fact that all the orbits have fixed-point attractors.

When it comes to the limiting configuration of *HK* systems, the $2R$-conjecture stands out as the most intriguing hypothesis. The concept of equilibrium stability was introduced in [3] to put this conjecture on formal grounds. Extensive experiments were conducted, suggesting a value closer to $2.2R$.

All the work cited so far considers only the deterministic version of the system. For the noisy version of the model, Pineda et al. consider a discrete-time formulation where, at each step, every agent randomly chooses to perform the usual *HK* step or to move randomly [29]. Two types of random jumps are considered: bounded jumps confine agents to a bounded distance from their current position while free jumps allow them to move anywhere. An approximate density-based master equation was developed for the analysis of the order-disorder phase transition and the noisy *HK* system was compared with another famous opinion dynamics system, the so-called *DW* model [11].

Consensus analysis of opinion systems can be found in [15]. In their work, Garnier et al. conduct linear stability analysis for the mean-field limiting equation for a group of opinion systems from [27]. Following this approach, the authors were able to determine whether the system achieves consensus (ie, a single-cluster state) for a given interaction kernel and noise level. Different types of kernels from [17,27] were considered and the results were further confirmed by extensive simulations.

A fairly technical L_1 analysis of the mean-field limiting equation for the noisy *HK* model was conducted in [9]. Well-posedness (ie, the existence, uniqueness, and non-negativity of the solution) was established along with an extensive discussion of regularity issues. Following this track, the authors conducted a global stability analysis of the system and exhibited an unstable zone for clustered profiles. In the present paper, a forbidden zone for disordered phase is obtained by linear stability analysis. Combining the two results above yields a possible co-existence region for clustered and disordered phases.

We now highlight the contributions of this paper. For the stochastic differential equation model of the noisy *HK* system, we propose an order parameter for analyzing the system behavior. The phase diagram of the system with respect to interacting range and noise level is outlined and phase transitions are observed when the interacting range is comparably small relative to the system size. For the clusters emerged from the dynamics, we are able to analyze the dependency of cluster width on the population and noise level. For the partial differential equation model induced from the mean-field limit of the SDE model, we prove that the cluster has a Gaussian profile under first-order approximation with respect to noise level. We describe a pseudo-spectral method for simulating the system efficiently with sufficient accuracy. By conducting a linear stability analysis, not only can we derive a

satisfactory theoretical explanation for the $2R$ conjecture, but we can also delineate the noise level corresponding to stable disordered phases in higher dimensions.

3 The Model

The stochastic differential equation (SDE) model we use in this paper can be expressed as

$$dx_i = -\frac{1}{N} \sum_{j:|x_i - x_j| \le R} (x_i - x_j)\, dt + \sigma\, dW_t^{(i)}, \tag{1}$$

where $i = 1, 2, \ldots, N$ denotes the agents, σ specifies the magnitude of the noise and $W_t^{(i)}$ represent independent Wiener processes. For technical convenience, we impose periodic boundary conditions on (1) by taking each x_i modulo $L = 1$ and interpreting $|z|$ as $\min\{|z|, L - |z|\}$. Intuitively, the model mediates the tension between two competing forces: the summation in (1) represents an attracting force that pulls the agents together while the diffusion term keeps them active in Brownian motion. This can be compared to the use of two parameters in the noisy model of Pineda et al.: a noise intensity m determines the probability that an agent should move to the mass center of its neighbors (vs. moving randomly), and γ bounds the length of the jump [29]. In the continuous-time model, the pair (m, γ) reduces to a single parameter, namely the noise magnitude σ.

In the mean-field limit $N \to \infty$, Eq. (1) induces a nonlinear Fokker-Planck equation for the agent density profile $\rho(x, t)$ [15]:

$$\rho_t(x, t) = \left(\rho(x, t) \int (x - y)\rho(y, t)\mathbf{1}_{|y-x| \le R})\, dy \right)_x + \frac{\sigma^2}{2} \rho_{xx}(x, t). \tag{2}$$

The function $\rho(x, t)$ is the limiting density of $\rho^N(x, t) := \frac{1}{N} \sum \delta_{x_j(t)}(dx)$, as N goes to infinity, where $\delta_x(dx)$ denotes the Dirac measure with point mass at x. In this partial differential equation form, the second derivative term represents the diffusion process that flattens the density ρ. On the other hand, the first term represents the advection of the density caused by attraction. In higher dimensions, one just needs to replace the first derivative by a divergence operator and replace the second derivative by a Laplace operator. We will use bold letter to denote a vector or a point in higher dimensional space.

To derive (2) from Eq. (1), we consider the agent flux of a small piece of space Ω. The Brownian motion of infinitely many agents is equivalent to a diffusion process, which implies that the flux caused by the noise is $-\sigma \nabla \rho$. On the other hand, the attraction between agents causes a flow with velocity $\int_{|y-x| \le R} (y - x)\rho(y, t)\, dy$ at x; hence a net outflow equal to the derivative of $\rho(x, t) \int_{|y-x| \le R} (y - x)\rho(y, t)\, dy$. Eq. (2) follows immediately from mass conservation and the divergence theorem. Regarding the boundary condition, none is necessary if we consider the system on the real line. For the case of an interval, we use Neumann boundary conditions, in this case a reflecting boundary condition since the flux at the boundary should be zero. In the case of different rules other than the *HK* rule or the case of external force, the corresponding mean-field equations will be of the same type of advection-diffusion equation with different kernels in the convolution. To simplify our analysis and simulation, we use a periodic boundary condition over the unit interval for the rest of this paper. Equivalently, the system can be regarded on a circle with unit perimeter.

4 System Dynamics and Phase Transitions

As we mentioned earlier, the original *HK* system always converges within a number of steps and the final configuration consists of a union of clusters with pairwise distance larger than R. A case of particular interest is that of a single cluster, forming what is commonly called *consensus*. Of course, when noise is added to the system, there is no "final" state to speak of; nevertheless, for the SDE model, one could focus on the averaged long-time behavior of the system as measured by the number of clusters. Intuitively, a higher noise level σ should correspond to more diffused clusters while, for σ above a certain threshold, clusters should break apart and release the agents to move randomly in the unit interval. This intuition is confirmed by simulating (1) for different values of R and σ.

To describe the system quantitatively, we introduce the order parameter

$$Q(\boldsymbol{x}) := \frac{1}{N^2} \sum_{i,j=1}^{N} \mathbf{1}_{|x_i - x_j| \le R} \tag{3}$$

to measure the edge density of the communication graph. Obviously, $Q = 1$ when a consensus state is reached and it can be easily checked that $Q = 2R/L$ when the agents are uniformly spread (disordered phase).

We highlight two interesting scenarios in the SDE model. For small values of σ, a random initial distribution of the agents evolves in the following manner: at the beginning, the attracting forces dominate and break symmetry by forming several clusters. As the clusters are formed, the noise term gradually overtakes the dynamics and produces a jiggling motion of the clusters. The mass center of the clusters follows a Brownian motion of variance σ^2/n, where n is the number of agents in the cluster. Brownian motion in one (and two) dimension(s) is recurrent so, as one would expect, the clusters formed in the early stage will eventually merge almost surely. Such merging process and the corresponding order parameter can be observed in Fig. 1 (with the time axis suitably transformed to make the evolution more apparent).

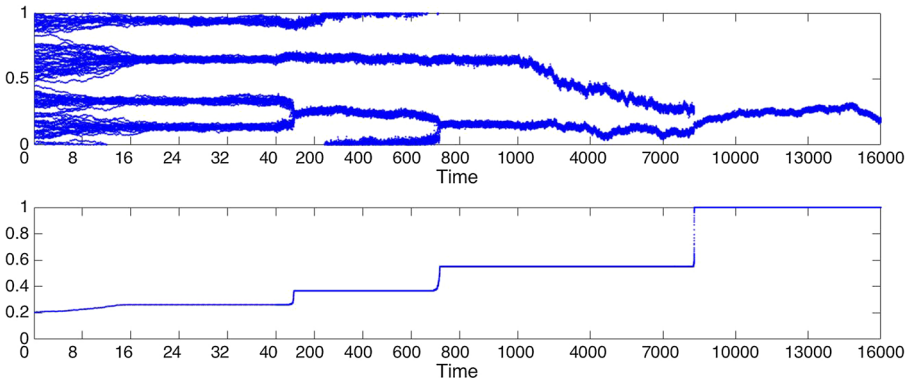

Fig. 1 (*Upper*) Simulation of the SDE model for noisy *HK* system with $n = 100$, $\sigma = 0.05$ and $R = 0.1$. At the beginning, several clusters are formed from the random distributed initial profile and later merge with each other. (*Lower*) The curve of the order parameter Q as a function of the time. Q starts at $2R/L = 0.2$ and then gradually increases during the process of cluster formation. Then Q jumps up for several times during cluster merging, and finally reaches 1, which represents the single cluster phase. The time axes in both figures are suitably transformed to make the evolution more apparent

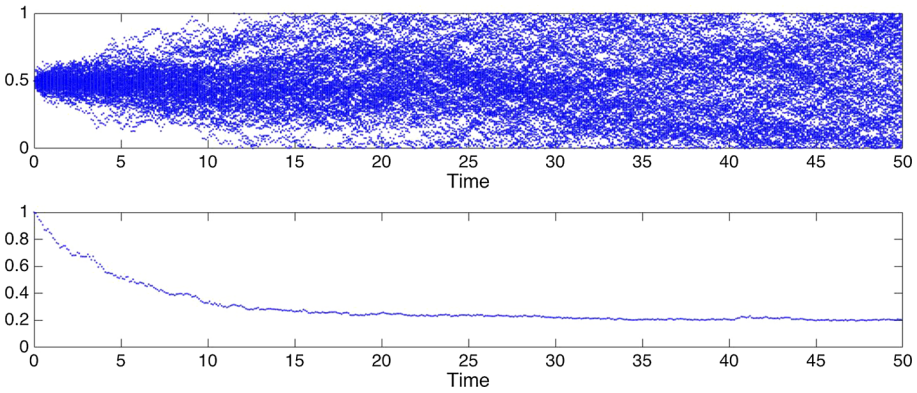

Fig. 2 (*Upper*) Simulation of a noisy *HK* system with $n = 100$, $\sigma = 0.07$ and $R = 0.1$. All the agents start at $x = 0.5$ and then diffuse to fill up the space. (*Lower*) The plot of the order parameter Q as a function of the time. Q stats at 1 and then gradually decreases during the diffusion and finally reaches the disordered state, in which case $Q = 2R/L = 0.2$

If σ is comparably large and we initialize the system by placing all the agents at the same position at $x = 0.5$, then the initial cluster breaks apart to fill up the entire space, as shown in Fig. 2. Notice that the order parameter Q decreases gradually from 1 to 0.2, which correspond to the single cluster state and the disordered state.

To better understand the collective behavior of the system, we carefully calculated the time-averaged order-parameter for different parameter pairs (R, σ) in the region $[0, 0.35] \times [0, 0.17]$ in the thermodynamic limit. We note here that in the discussion of phase transition phenomena of the *HK* model, the thermodynamic limit we consider is the limit $N \to \infty$ with the box size L fixed. This is different from the usual thermodynamic limit in statistical mechanics where one has $N \to \infty$, $L \to \infty$ with the density N/L fixed and finite. The resulting phase diagram is demonstrated in Fig. 3. For each parameter point in Fig. 3, a system with $N = 300$ agents is simulated for sufficiently long time (T = 105). The initial profile is randomly sampled from uniform distribution, and the time-averaged order parameter is calculated within the time period when the system has reached a steady state. Figure 3 suggests that $Q(\boldsymbol{x})$ is discontinuous near the origin, signifying the presence of a first order phase transition. The first order transition line does not persist indefinitely and vanishes for large R. This is because when the interval length R is large, the noise level σ need to be comparably large to overcome the attracting forces among the agents. The distinction between the clustered phase and the disordered one hence becomes blurry for large (R, σ) and the phase transition ceases to be observable. This is the region where the boundary effect comes up.

We choose two groups of parameters (R, σ) to demonstrate the behavior of the system (Fig. 4). The first group contains $(R, \sigma) =$ (A)$(0.05, 0.01)$, (B)$(0.05, 0.02)$, and (C)$(0.05, 0.03)$, which are close to the origin. It can be observed that at (A), a single, narrow cluster is formed doing Brownian motion. When the noise level increases to (B), some agents are able to escape the cluster to travel around the entire domain. The cluster itself is still visible. For even larger level of noise at (C), the cluster disappears, and agents move disorderly. For parameters away from the origin at $(R, \sigma) =$ (D)$(0.2, 0.07)$, (E)$(0.2, 0.09)$, and (F)$(0.2, 0.11)$, the transition from clustered state to disordered state still exists but is more difficult to observable. In general, clusters widen as σ grows. This observation will be explained in Section 5.

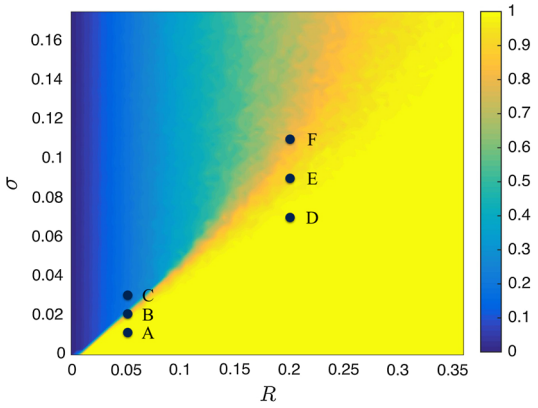

Fig. 3 Phase diagram for the SDE model. The *color scale* represents the value of order parameter $Q(\boldsymbol{x})$ as defined in Eq. (3). The domain size $L = 1$, number of agents $N = 300$, and time $t = 10^5$, the latter being large enough to ensure that the system has reached steady state. The value of the order parameter is calculated as the time average of $Q(\boldsymbol{x})$ after the system becomes steady. We note the existence of a phase transition for small σ consisting of a line separating clustered and disordered states. The transition line vanishes at higher noise level. We highlight two groups of parameter points (A, B, C) and (D, E, F) shown in the figure. The corresponding dynamics are shown in Fig. 4 (Color figure online)

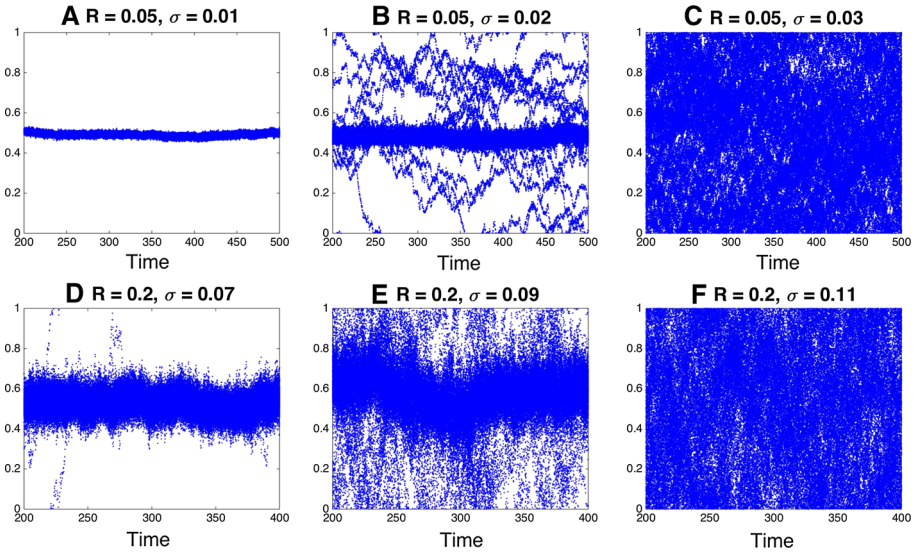

Fig. 4 Simulations of six independent systems: $R = 0.05, \sigma = 0.01$(A), 0.02(B), 0.03(C) in the time window [200, 500]; and $R = 0.2$, $\sigma = 0.07$(D), 0.09(E), 0.11(F) in the time window [200, 400]. For visualizing purposes, only 100 randomly chosen agents are plotted to avoid saturation, and the diagram is shifted to keep the cluster around the center. The positions of the parameter pairs in the phase diagram are shown in Fig. 3

The periodic boundary condition we adopted helps the agents escaped from the cluster to be absorbed back. This is because the escaped agents can come back from either side of the cluster. For the noisy *HK* system on the real line, on the other hand, it is much more difficult for escaped agents to join the cluster again since the random walk will be null-recurrent [28].

5 Analysis of the Clustered Phase

We analyze the long-time profile of the clustered phase with respect to the interval length R and the noise level σ. An important difference with the original noiseless *HK* system is that clusters do not form single points but evolving intervals of moving points. We seek conditions on (R, σ) to make the clusters stable.

5.1 The Clustered Phase in the SDE Model

If we assume that the widths of the clusters are smaller than $2R$, then the drift term becomes simpler. Indeed, suppose there are n agents in the cluster and let $g(t) = \frac{1}{n}\sum_{i=1}^{n} x_i(t)$ denote the center of mass. The equations for $x_i(t)$ and $g(t)$ become $dx_i = \frac{n}{N}(g(t) - x_i)\,dt + \sigma\, dW_t^{(i)}$ and $dg = \frac{\sigma}{n}\sum_{i=1}^{n} dW_t^{(i)}$. Then it is straightforward to see that

$$dx_i = -\frac{n}{N} x_i\, dt + \sigma\, dW_t^{(i)} + \frac{\sigma}{N}\sum_{k=1}^{n} dW_t^{(k)}. \tag{4}$$

Pick one cluster and assume that all of its agents are initially placed at the origin. They will oscillate in Brownian motion while being pulled back to the origin because of the first term of (4). It follows that the invariant measure of the stochastic differential equation above provides a faithful description of the local profile. Since the SDE (4) is linear in $\boldsymbol{x} = (x_1, \ldots, x_n)$ and the diffusion term is constant, it describes a Gaussian process; therefore, it suffices to study the first two moments of the vector $\boldsymbol{x}$ to provide its complete characterization in distribution. Using Itô calculus, we obtain the following moment equations:

$$\begin{aligned} d\mathbb{E}x_i &= -\frac{n}{N}\,\mathbb{E}x_i\, dt\,, \\ d\mathbb{E}x_i x_j &= \left(-\frac{2n}{N}\,\mathbb{E}x_i x_j + \sigma^2(\Sigma\Sigma^T)_{ij}\right) dt, \end{aligned}$$

where $\Sigma_{ij} = \frac{1}{N} + \delta_{ij}$. This implies that

$$\mathbb{E}x_i x_j = \frac{N\sigma^2}{2n}(\Sigma\Sigma^T)_{ij}(1 - e^{-2nt/N}).$$

Hence, at steady state,

$$\mathbb{E}x_i = 0 \qquad \text{and} \qquad \mathbb{E}x_i x_j = \frac{N\sigma^2}{2n}(\Sigma\Sigma^T)_{ij}.$$

This implies a Gaussian profile at steady state of the form $x_i \sim \mathcal{N}(0, \frac{N\sigma^2}{2n}\Sigma\Sigma^T)$. If we use M to denote the all-one matrix, then $\Sigma = I + \frac{1}{N}M$. Hence the covariance matrix

$$Var(\boldsymbol{x}) = \frac{N\sigma^2}{2n}\Sigma\Sigma^T = \frac{N\sigma^2}{2n}\left(I + \left(\frac{2}{N} + \frac{n}{N^2}\right)M\right). \tag{5}$$

Notice that the covariance matrix $\frac{N\sigma^2}{2n}\Sigma\Sigma^T$ has one-fold eigenvalue $(1 + \frac{n}{2N} + \frac{N}{2n})\sigma^2$ and $(n-1)$-fold eigenvalue $\frac{N\sigma^2}{2n}$. Therefore the cluster size depends linearly on σ. Furthermore, since these two eigenvalues both decrease when n increases from 1 to N, the cluster size actually increases as the number of agents declines. This result may seem counterintuitive at a first glance because more agents are naturally associated with larger clusters. In the SDE

model, however, more agents lead to stronger attraction to the mass center, which results in smaller-size clusters.

5.2 The Clustered Phase in the PDE Model

In this part, we will establish an asymptotic solution of clustered phase for small σ. Concretely, our solution $\rho_0(x)$ is defined as

$$\rho_0(x) = Ce^{-\min\{x^2, R^2\}/\sigma^2}, \tag{6}$$

where the normalization constant C ensures summation to 1. Notice that any translation of ρ_0 in x-direction is also an asymptotic solution.

The clustered phase corresponds to a steady solution of (2). We assume that the clustered phase is stable for the given parameters R and σ. In addition, we focus on the case where R is much smaller than $L = 1$, otherwise the clustered phase is not stable. By (2), the steady-state equation can be expressed as

$$\left(\rho(x)\int_{x-R}^{x+R}(y-x)\rho(y)\,dy\right)' = \frac{\sigma^2}{2}\rho''(x). \tag{7}$$

After integrating the above equation once, we have

$$\rho(x)\int_{x-R}^{x+R}(y-x)\rho(y)\,dy = \frac{\sigma^2}{2}\rho'(x) + C_1. \tag{8}$$

Note that $\rho(x) \equiv 1$ is a solution for $C_1 = 0$. For a single-cluster profile, we may assume without loss of generality that the cluster is centered around 0 and the solution is symmetric: $\rho(x) = \rho(-x)$. By periodicity, we can confine our analysis to the interval $[-1/2, 1/2]$, which implies $C_1 = 0$. Rearranging and integrating (8) once more yields

$$\rho(x) = \rho(0)\exp\left\{\frac{2}{\sigma^2}\int_{-1/2}^{1/2}K(x,y)\rho(y)\,dy\right\}, \tag{9}$$

where

$$K(x,y) = \int_0^x (y-\xi)\,\mathbf{1}_{|y-\xi|\le R}\,d\xi. \tag{10}$$

It is easy to evaluate the kernel K. For $|x| > 2R$, we have

$$K(x,y) = \begin{cases} \frac{1}{2}(R+x-y)(R-x+y) & x-R \le y \le x+R, \\ \frac{1}{2}(y^2-R^2) & -R \le y \le R, \\ 0 & \text{otherwise.} \end{cases} \tag{11}$$

For $0 \le x \le 2R$, we get

$$K(x,y) = \begin{cases} \frac{1}{2}(R+x-y)(R-x+y) & R \le y \le x+R, \\ -\frac{1}{2}x(x-2y) & x-R \le y \le R, \\ \frac{1}{2}(y^2-R^2) & -R \le y \le x-R, \\ 0 & \text{otherwise.} \end{cases} \tag{12}$$

and for $-2R \le x < 0$, we get

$$K(x, y) = \begin{cases} \frac{1}{2}(R + x - y)(R - x + y) & x - R \le y \le -R, \\ -\frac{1}{2}x(x - 2y) & -R \le y \le x + R, \\ \frac{1}{2}(y^2 - R^2) & x + R \le y \le R, \\ 0 & \text{otherwise.} \end{cases} \tag{13}$$

It is not easy to solve the integral functional equation (9) for ρ directly. We will show that ρ_0 defined in (6) solves (9) up to the leading term in the expansion in σ. Observe that, for σ much smaller than R, the profile ρ_0 is concentrated around $x = 0$, so we only need to evaluate the integral in (9) near $y = 0$ and thus ignore error terms exponentially small in σ. For $|x| \le R$, by (12, 13), we see that near $y = 0$,

$$K(x, y) = -\frac{1}{2}x(x - 2y). \tag{14}$$

The exponent on the right hand side of (9) becomes

$$\begin{aligned} \frac{2}{\sigma^2}\int_{-1/2}^{1/2} K(x, y)\,\rho_0(y)\,dy &= -\frac{1}{\sigma^2}\int_{-1/2}^{1/2} x(x - 2y)\rho_0(y)\,dy \\ &= -\frac{x^2}{\sigma^2}\int_{-1/2}^{1/2} \rho_0(y)\,dy = -\frac{x^2}{\sigma^2}, \end{aligned}$$

which satisfies (9). On the other hand, for $|x| > R$, near $y = 0$, we have

$$K(x, y) = \frac{1}{2}(y^2 - R^2). \tag{15}$$

Thus,

$$\frac{2}{\sigma^2}\int_{-1/2}^{1/2} K(x, y)\,\rho_0(y)\,dy = \frac{1}{\sigma^2}\int_{-1/2}^{1/2} (y^2 - R^2)\rho_0(y)\,dy = -\frac{R^2}{\sigma^2} + O(\sigma).$$

Once again, (9) is satisfied, this time up to the leading term in the expansion in σ. We have thus established that, in the presence of a low level of noise, the single-cluster steady state has a Gaussian profile with variance $\sigma^2/2$ near the cluster with exponential error decay as function of σ. Notice that convex combinations of cluster profiles of the form (6) but centered at different locations in (7) generate error terms in $O(\sigma)$ as long as the distances between clusters are large enough to eliminate inter-cluster interaction. As a result, multiple Gaussians are also steady-state solutions in the σ-error sense as long as the Gaussians are well-separated. The asymptotic solution (6) matches remarkably well the simulation results for the PDE model given in the next subsection.

5.3 Simulation for the PDE Model

To simulate the Fokker-Planck Eq. (2), we adopt the well-known pseudo-spectral method. Pseudo-spectral method has been extensively used for simulating PDEs with with periodic boundaries, especially in the fields of fluid dynamics and material science [13,19]. In our case, the advection term of (2) is easy to calculate in the real space, while it is more convenient to calculate the diffusion term in Fourier space. Therefore by using Fast Fourier Transform,

(2) can be efficiently solved numerically. We expand $\rho(x,t)$ in Fourier space and cut off the expansion at m (L is assumed to be 1 without loss of generality):

$$\rho(x,t) \approx \sum_{k=-m}^{m} \hat{\rho}_k(t) e^{i2\pi kx}. \tag{16}$$

Then the integral in (2) can be carried out explicitly as

$$\begin{aligned}
&\int_{x-R}^{x+R} (y-x)\rho(y,t)\,dy \\
&= \int_{-R}^{R} y\rho(x+y,t)\,dy \approx \sum_{k=-m}^{m} \hat{\rho}_k(t) e^{i2\pi kx} \int_{-R}^{R} y e^{i2\pi ky}\,dy \\
&\approx \sum_{-m\le k\le m, k\neq 0} \left\{ \frac{R}{i2\pi k}\left(e^{i2\pi kR} + e^{-i2\pi kR}\right) \right. \\
&\quad \left. + \frac{1}{4\pi^2 k^2}\left(e^{i2\pi kR} - e^{-i2\pi kR}\right) \right\} \hat{\rho}_k(t) e^{i2\pi kx}.
\end{aligned}$$

The above formula can also be interpreted as the Fourier transform of the convolution of the density $\rho(x,y)$ and the kernel $x\mathbf{1}_{|x|\le R}$, which equals the product of the Fourier transform of the density and the Fourier transform of the kernel. However, it is more convenient to conduct the multiplication of the integral and $\rho(x,t)$ in the real space, thus we use inverse Fourier transform to get the convolution back to the real space. Finally, the first and second derivative will be calculated in the Fourier space by using Fourier transform one more time. As for the time direction, we discretize the density as $\hat{\rho}_{k,r} = \hat{\rho}_k(rh)$. Since the second derivative term (or the Laplacian term in higher dimensions) is linear in ρ but the first term is not, we could use a semi-implicit scheme to improve the accuracy of the algorithm. The numerical scheme is summarize in Algorithm 1. Notice that the conservation of mass $\int \rho(y,t)\,dy = 1$

Algorithm 1 A semi-implicit pseudo-spectral method for PDE (2)

For $r = 0$ to $T-1$

Conduct *FFT*: $\rho_{k,r} \xrightarrow{\text{FFT}} \hat{\rho}_{k,r}$

Calculate $\hat{\varphi}_{k,r} := \left[\frac{R}{i2\pi k}(e^{i2\pi kR} + e^{-i2\pi kR}) + \frac{1}{4\pi^2 k^2}(e^{i2\pi kR} - e^{-i2\pi kR})\right]\hat{\rho}_{k,r}$

Conduct inverse *FFT*: $\hat{\varphi}_{k,r} \xrightarrow{\text{iFFT}} \varphi_{k,r}$

Calculate the product $\psi_{k,r} := \varphi_{k,r}\rho_{k,r}$

Conduct *FFT*: $\psi_{k,r} \xrightarrow{\text{FFT}} \hat{\psi}_{k,r}$

Semi-implicit update: $\hat{\rho}_{k,r+1} = \left(-i2\pi k\hat{\psi}_{k,r} - 2\pi^2\sigma^2 k^2 \hat{\rho}_{k,r+1}\right)h + \hat{\rho}_{k,r}$

Set $\hat{\rho}_{0,r+1} = \hat{\rho}_{0,r}$ and conduct inverse *FFT*: $\hat{\rho}_{k,r+1} \xrightarrow{\text{iFFT}} \rho_{k,r+1}$

is automatically satisfied in Eq. (2); therefore we only need to set $\hat{\rho}_{0,r+1} = \hat{\rho}_{0,r}$ during the iteration to prevent the cumulation of numerical error while no further treatment is required.

During the simulations, the initial profile is chosen to be Gaussian $C \times e^{-20(x-0.5)^2}$, where the constant C rescales the density to ensure that the total mass is equal to 1. As demonstrated in Fig. 5, the interaction range $R = 0.2$, and σ has four different values 0.1, 0.15, 0.2, 0.25. It can be observed that for smaller σ, the system will evolve to reach a clustered profile. In addition, in the case when σ is larger, the cluster is shorter and wider. When σ goes beyond

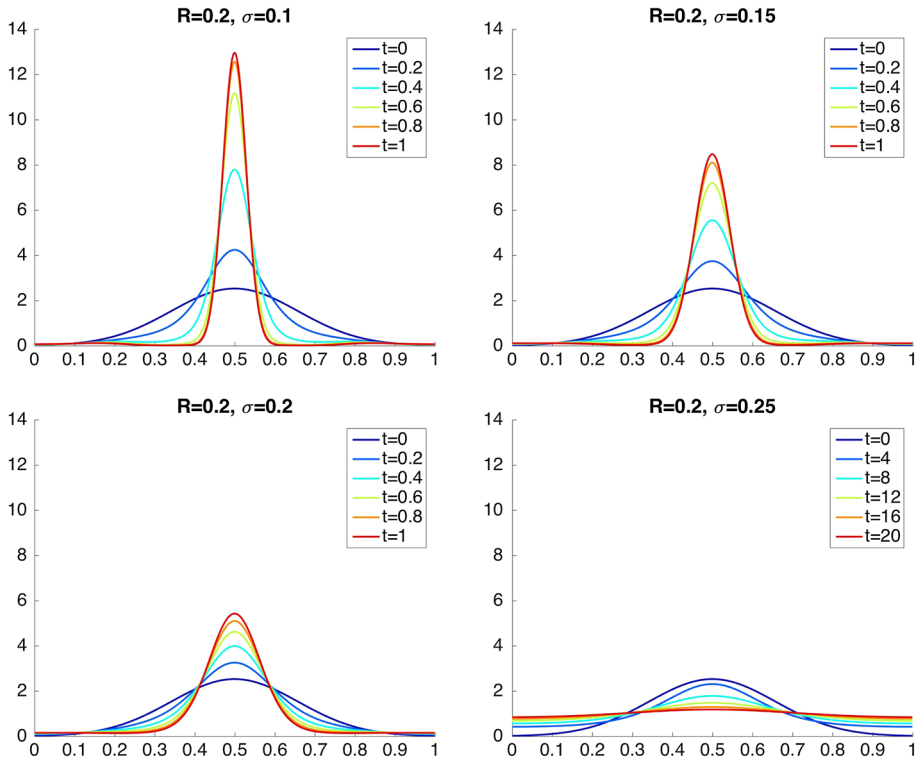

Fig. 5 Simulations of Eq. (2) for $R = 0.2$ and $\sigma = 0.1, \sigma = 0.15, \sigma = 0.2$ and $\sigma = 0.25$. The initial value is set as $\rho(x, 0) \propto e^{-20(x-0.5)^2}$. The density profile of the system at different time is indicated by curves with *different colors* (Color figure online)

a certain value, the system no longer evolves into a clustered profile; instead, the density flattens to a straight line, which corresponds to the disordered phase.

It is worth mentioning that directly simulating the SDE model will suffer a second order complexity $O(N^2)$ with respect to the number of agents. This is because the interaction between any pair of agents contributes to the dynamics of the system. On the other hand, for noisy *HK* systems with a large number of agents, directly simulating the Fokker-Planck Equation (2) achieves better computational efficiency since Eq. (2) is density-based and thus is independent with the number of agents.

6 The Disordered Phase and the $2R$-Conjecture

In order to find the region where the disordered phase is stable, we conduct linear stability analysis with ansatz $\rho(\boldsymbol{x}, t) = 1 + p(t)e^{2\pi i \boldsymbol{k}\cdot\boldsymbol{x}}$ ($\boldsymbol{k} = (k_1, k_2, \ldots, k_d)$) to the mean-field Fokker-Planck equation in dimension d with periodic boundary conditions in the unit cube (that is, reducing each coordinate modulo $L = 1$):

$$\frac{\partial}{\partial t}\rho(\boldsymbol{x}, t) = \nabla \cdot \left(\rho(\boldsymbol{x}, t) \int_{\|\boldsymbol{x}-\boldsymbol{y}\| \le R} (\boldsymbol{x} - \boldsymbol{y})\rho(\boldsymbol{y}, t)\, d\boldsymbol{y} \right) + \frac{\sigma^2}{2}\Delta\rho(\boldsymbol{x}, t),$$

with the initial value $\rho(\boldsymbol{x}, 0) = \rho_0(\boldsymbol{x})$ and under the constraint $\int_0^1 \rho(\boldsymbol{x}, t)\, d\boldsymbol{x} = 1$. The main idea behind the linear stability analysis is that we give the uniform solution $\rho(\boldsymbol{x}, t) = 1$ a small perturbation, obtain a linear differential equation for $p(t)$ by ignoring its higher order terms, and see whether the magnitude of the perturbation, $p(t)$, will amplify or vanish. The fact that $p(t)$ will amplify is sufficient for the disordered phase to be unstable, since being stable means that the disordered state is resistant to any kinds of perturbation. Gram-Schmidt orthogonalization guarantees that we could find an orthogonal matrix M such that the first row of M is $\boldsymbol{k}/K$, where $K := \|\boldsymbol{k}\|_2$. By defining $\boldsymbol{z} = M\boldsymbol{y}$, we then have $z_1 = \boldsymbol{k} \cdot \boldsymbol{y}/K$. Now let $s = 2\pi K R$ and plug in the ansatz $\rho(\boldsymbol{x}, t) = 1 + p(t)e^{2\pi i \boldsymbol{k}\cdot\boldsymbol{x}}$. For p small enough, this gives us

$$\begin{aligned}
&p_t e^{2\pi i \boldsymbol{k}\cdot\boldsymbol{x}} \\
&= -\nabla \cdot \left((1 + pe^{2\pi i \boldsymbol{k}\cdot\boldsymbol{x}}) \int_{\|\boldsymbol{y}\|\le R} \boldsymbol{y} p e^{2\pi i \boldsymbol{k}\cdot(\boldsymbol{x}+\boldsymbol{y})}\, d\boldsymbol{y} \right) \\
&\quad -2\pi^2\sigma^2 K^2 p e^{2\pi i \boldsymbol{k}\cdot\boldsymbol{x}} \\
&\approx -2\pi i p e^{2\pi i \boldsymbol{k}\cdot\boldsymbol{x}} \int_{\|\boldsymbol{y}\|\le R} \boldsymbol{k}\cdot\boldsymbol{y} e^{2\pi i \boldsymbol{k}\cdot\boldsymbol{y}}\, d\boldsymbol{y} - 2\pi^2\sigma^2 K^2 p e^{2\pi i \boldsymbol{k}\cdot\boldsymbol{x}} \\
&\approx -2\pi i p e^{2\pi i \boldsymbol{k}\cdot\boldsymbol{x}} \int_{\|\boldsymbol{z}\|\le R} K z_1 e^{2\pi i K z_1}\, d\boldsymbol{z} - 2\pi^2\sigma^2 K^2 p e^{2\pi i \boldsymbol{k}\cdot\boldsymbol{x}} \\
&\approx sRp e^{2\pi i \boldsymbol{k}\cdot\boldsymbol{x}} \int_{\|\boldsymbol{z}\|\le 1} z_1 e^{isz_1}\, d\boldsymbol{z} - 2\pi^2\sigma^2 K^2 p e^{2\pi i \boldsymbol{k}\cdot\boldsymbol{x}}\,.
\end{aligned}$$

This results in the ODE

$$p_t = R\left(s \int_{\|\boldsymbol{z}\|\le 1} z_1 \sin(sz_1)\, d\boldsymbol{z} - \frac{\sigma^2}{2R^3} s^2 \right) p = 2Rp \left(\frac{\sin s}{s} - \cos s - \frac{\sigma^2}{4R^3} s^2 \right).$$

In dimension $d = 1$, the ODE reduces to $p_t/p = 2Rf_\gamma(s)$, where $\gamma := \sigma^2/4R^3$ and $f_\gamma(s)$ is defined as

$$f_\gamma(s) = \frac{\sin s}{s} - \cos s - \gamma s^2. \tag{17}$$

When $f_\gamma(s) \le 0$ for all $s = 2k\pi R$, small perturbation to $\rho = 1$ will decay and finally vanish. On the other hand, if some k makes $f_\gamma(s) > 0$, then $\rho = 1$ is no longer stable and the system yields a clustered phase. Since its first two terms in (17) are bounded, $f_\gamma(s) < 0$ for all $s > s_0$ and $\gamma > 0$, which means that the high frequency modes are all stable. On the other hand, when $\gamma = 0$ (the noiseless model), $f_\gamma(s)$ behaves like $-\cos s$ for s large enough, which implies that $f_\gamma(s)$ can be positive for infinitely many frequencies. When $\gamma > 0.012$, $f_\gamma(s) > 0$ only over an interval of the form $[0, s_1]$, corresponding to the low frequency modess. As γ increases, s_1 shrinks to become nearly 0 at $\gamma = \frac{1}{3}$. The behavior of $f_\gamma(s)$ for different values of γ is shown in Fig. 6.

6.1 The Unstable Zone for the Disordered Phase

When the noise level σ is very small, the clustering effect of the system dominates and the system falls within the clustered phase. Taylor expansion of $f_\gamma(s)$ shows that it can take on positive values as long as $\gamma < \frac{1}{3}$, which gives us the critical curve $\sigma^2 = \frac{4}{3}R^3$. The boundary is accurate when R is small enough, since a suitable frequency k can always be found such that $f_\gamma(s) > 0$, hence making the disordered phase unstable. Conversely, for large R, $f_\gamma(s)$ could be negative for all k, conferring stability, even though $f_\gamma(s) > 0$ for some $s < 2\pi R$.

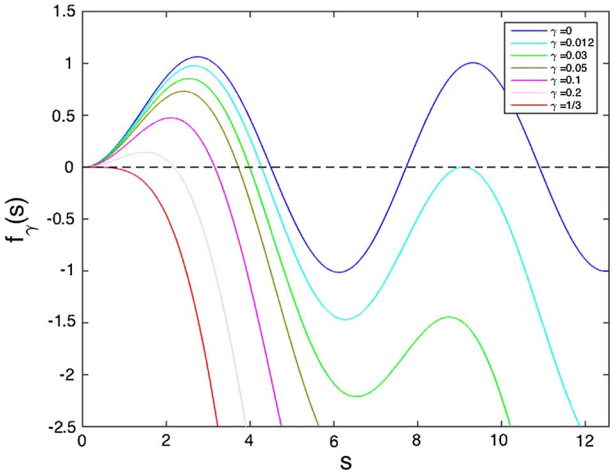

Fig. 6 The profile of function $f_\gamma(s)$ for different values of γ

Below the critical curve $\sigma^2 = \frac{4}{3}R^3$ lies the unstable zone for the disordered phase in which symmetry breaking fragments the constant solution $\rho = 1$ into separate clusters. This curve is further validated by the simulation results in Section 5.3. It can be observed, by combining Fig. 3 and the formula $\sigma^2 = \frac{4}{3}R^3$, that the disordered-clustered boundary from the simulation lies a little above the critical curve obtained in this section.

6.2 Supporting the $2R$ Conjecture

The conjecture in questions refers to the original (noiseless) *HK* model: it states that, if the agents starts out uniformly distributed in [0, 1], they will converge toward clusters separated by distance of roughly $2R$, thus setting their number close to the value $1/2R$. This assumes that N and $1/R$ are large enough. To address this conjecture in the PDE model, we must confine γ to the range $[0, \frac{1}{3}]$ to make the clustered phase stable and then ask how many clusters one should expect.

We first rule out the case $s > 2\pi$ by considering the pairwise distance of the resulting clusters. Notice that when $s > 2\pi$, k is then larger than $1/R$. Even if the wave $e^{2\pi ikx}$ grows, it cannot exist for too long since the pairwise distance of the clusters would be smaller than R. Therefore for this class of waves, no matter whether they are initially stable or unstable during the perturbation, they will not contribute to the final profile of the system. Then it is safe to focus on the interval $s \in [0, 2\pi]$. The expected number of clusters is given by the value of s that maximizes $f_\gamma(s)$. Numerical calculation shows that the root of $f'_\gamma(s) = 0$ (the peak's location) shifts to the left as γ grows from 0 to $\frac{1}{3}$. This implies that the number of clusters $k = s/(2\pi R)$ decreases as the noise level rises. The $2R$ conjecture corresponds to the case $\gamma = 0$. Numerical calculation indicates that the smallest nonzero root of $f'_0(s)$ is $s^* = 2.7437$. It follows that the expected number of final clusters is equal to

$$k^* = \frac{s^*}{2\pi R} = \frac{1}{2.29R}.$$

Note that the bound comes fairly close to the number observed experimentally for *HK* systems with a finite number of agents [3].

6.3 The Higher-Dimensional Case

In higher dimensions, we have to consider functions of the form

$$F_\gamma(s) := \frac{1}{2}s\int_{\|z\|\le 1} z_1 \sin(sz_1)\,dz - \gamma s^2.$$

For the forbidden zone of the disordered phase, we can use a Taylor expansion for F_γ in s to determine the critical noise level σ for a given R. Let S_{d-1} denote the area of the unit sphere in dimension d. It is well known that $S_1 = 2\pi$ and $S_2 = 4\pi$. For general d, we have

$$S_{d-1} = \frac{2\pi^{d/2}}{\Gamma(\frac{d}{2})}, \quad \text{where } \Gamma(s) := \int_0^\infty x^{s-1}e^{-x}\,dx.$$

It follows that

$$\begin{aligned} F_\gamma(s) &\approx \frac{1}{2}s\int_{\|z\|\le 1} sz_1^2\,dz - \gamma s^2 \approx \frac{s^2}{2d}\int_{\|z\|\le 1}\|z\|^2\,dz - \gamma s^2 \\ &\approx \frac{s^2}{2d}\int_0^1 S_{d-1}r^{d+1}\,dr - \gamma s^2 \approx \left(\frac{\pi^{d/2}}{d(d+2)\Gamma(\frac{d}{2})} - \gamma\right)s^2. \end{aligned}$$

The above expansion gives us the boundary at which the disordered phase loses stability:

$$\sigma^2 = \frac{4\pi^{d/2}}{d(d+2)\Gamma(\frac{d}{2})}R^3.$$

Notice that the right-hand side equals $\frac{\pi}{2}R^3 > \frac{4}{3}R^3$ when $d = 2$, which means that in two dimensions we need even larger noise to make the disordered phase stable. As the dimension grows, however, the Gamma function will bring the noise level down to zero and the disordered phase will dominate unless the system becomes essentially noiseless.

7 Discussions

In the SDE model, simulations in Section 4 indicate that only a single-cluster profile survives the merging process, provided that the noise level is suitably low. Multiple-cluster profile will eventually disappear and is hence unstable. In contrast, the multiple-cluster profile can be stable in the PDE model, as demonstrated in the simulation results in Section 5.3. We note that the difference originates from the different scenarios that each model applies to. The SDE model works on systems with finite agents. In this case, clusters merge into one under the long-time limit ($t \to \infty$). On the other hand, the PDE model is obtained by taking the thermodynamic limit on any fixed time interval $[0, t]$. The multiple-cluster state then appears in long-time simulation for the PDE. Essentially, we observe multiple clusters by taking the mean-field limit ($N \to \infty$) first and the long-time limit ($t \to \infty$) afterwards. An alternative understanding is that, for the emergence of the single-cluster profile, the SDE requires longer time for increasing number of agents. The PDE is for infinite agents, and thus clusters may never merge in finite time.

The PDE model is suitable for a system with truly large number of agents over non-exponentially-large timescales. The SDE model, on the other hand, is a good approximation for systems with a finite number of agents over any time scales. In statistical physics, it is not uncommon that the order in which two limits are taken matters greatly; for example, in the

Ising model, taking the thermodynamic limit and bringing the magnetic field to zero must be performed in that order so as to obtain the desired result. This work provides yet another example of this phenomenon.

8 Conclusions

The contribution of this paper is an analysis of the clustering modes of the noisy Hegselmann-Krause model. We have provided theoretical insights, validated by numerical simulations, into the stochastic differential equation model for a finite number of agents and the Fokker-Planck model for the mean-field approximation in the thermodynamic limit. In the SDE model, we have shown that the system exhibits either disorder or single-cluster profile. We have proposed an order parameter based on the edges density of the communication graph to describe the phase transition. In the PDE model, we used linear stability analysis to find a forbidden zone for disordered phase in which the constant solution cannot survive in the long run. Most important, we provided a theoretical explanation for the $2R$ conjecture.

Acknowledgements We wish to thank the anonymous referees for many useful comments and suggestions. Bernard Chazelle's work is supported in part by NSF Grants CCF-0832797, CCF-0963825, and CCF-1016250; Weinan E's work is supported by DOE grant DE-SC0009248 and ONR grant N00014-13-1-0338; Qianxiao Li's work is supported by Agency for Science, Technology and Research, Singapore.

References

1. Axelrod, R.M.: The Evolution of Cooperation. Basic books, New York (2006)
2. Bhattacharyya, A., Braverman, M., Chazelle, B., Nguyen, H. L.: On the convergence of the Hegselmann-Krause system. In Proceedings of the 4th conference on Innovations in Theoretical Computer Science, pp. 61–66. ACM, New York (2013)
3. Blondel, V. D., Hendrickx, J. M., Tsitsiklis, J. N.: On the 2r conjecture for multi-agent systems. In Control Conference (ECC), 2007 European, IEEE, pp. 874–881 (2007)
4. Blondel, V.D., Hendrickx, J.M., Tsitsiklis, J.N.: On Krause's multi-agent consensus model with state-dependent connectivity. IEEE Trans. Autom. Control **54**(11), 2586–2597 (2009)
5. Castellano, C., Fortunato, S., Loreto, V.: Statistical physics of social dynamics. Rev. Mod. Phys. **81**(2), 591 (2009)
6. Chazelle, B.: The total s-energy of a multiagent system. SIAM J. Control Optim. **49**(4), 1680–1706 (2011)
7. Chazelle, B.: An algorithmic approach to collective behavior. J. Stat. Phys. **158**, 514–548 (2015)
8. Chazelle, B.: Diffusive influence systems. SIAM J. Comput. **44**(5), 1403–1442 (2015)
9. Chazelle, B., Jiu, Q., Li, Q., Wang, C.: Well-posedness of the limiting equation of a noisy consensus model in opinion dynamics. arXiv preprint arXiv:1510.06487 (2015)
10. Chazelle, B., and Wang, C.: Inertial Hegselmann-Krause systems. In Proceedings of the IEEE American Control Conference (ACC) , pp. 1936–1941. (2016)
11. Deffuant, G., Neau, D., Amblard, F., Weisbuch, G.: Mixing beliefs among interacting agents. Adv. Complex Syst. **3**, 87–98 (2000)
12. Easley, D., Kleinberg, J.: Networks, Crowds, and Markets: Reasoning About a Highly Connected World. Cambridge University Press, Cambridge, UK (2010)
13. Fornberg, B.: A Practical Guide to Pseudospectral Methods, vol. 1. Cambridge University Press, Cambridge, UK (1998)
14. Fortunato, S.: On the consensus threshold for the opinion dynamics of Krause-Hegselmann. Int. J. Mod. Phys. C **16**(02), 259–270 (2005)
15. Garnier, J., Papanicolaou, G., Yang, T.: Consensus convergence with stochastic effects. CoRR abs/1508.07313 (2015)
16. Hendrickx, J., Blondel, V.: Convergence of different linear and non-linear Vicsek models. In Proc. 17th Int. Symp. Math. Theory Networks Syst. (MTNS 2006), pp. 1229–1240. (2006)

17. Jabin, P.-E., Motsch, S.: Clustering and asymptotic behavior in opinion formation. J. Differ. Equ. **257**(11), 4165–4187 (2014)
18. Jadbabaie, A., Lin, J., Morse, A.S.: Coordination of groups of mobile autonomous agents using nearest neighbor rules. IEEE Trans. Autom. Control **48**, 988–1001 (2003)
19. Jiang, K., Wang, C., Huang, Y., Zhang, P.: Discovery of new metastable patterns in diblock copolymers. Commun. Computat. Phys. **14**: 443–460 (2013)
20. Kurz, S.: Optimal control of the freezing time in the Hegselmann-Krause dynamics. J. Differ. Equ. Appl. **21**(8), 633–648 (2015)
21. Lorenz, J.: A stabilization theorem for dynamics of continuous opinions. Phys. A **355**(1), 217–223 (2005)
22. Lorenz, J.: Consensus strikes back in the Hegselmann-Krause model of continuous opinion dynamics under bounded confidence. J. Artif. Soc. Soc. Simul. **9**(1), 8 (2006)
23. Martínez, S., Bullo, F., Cortés, J., Frazzoli, E.: On synchronous robotic networks — part II: time complexity of rendezvous and deployment algorithms. IEEE Trans. Autom. Control **52**(12), 2214–2226 (2007)
24. Martinsson, A.: An improved energy argument for the Hegselmann–Krause model. J. Differ. Equ. Appl, 1–6 (2015)
25. Mohajer, S., Touri, B.: On convergence rate of scalar Hegselmann-Krause dynamics. In Proceedings of the IEEE American Control Conference (ACC) (2013)
26. Moreau, L.: Stability of multiagent systems with time-dependent communication links. IEEE Trans. Autom. Control **50**(2), 169–182 (2005)
27. Motsch, S., Tadmor, E.: Heterophilious dynamics enhances consensus. SIAM Rev. **56**(4), 577–621 (2014)
28. Norris, J.R.: Markov Chains. Cambridge University Press, Cambridge, UK (1998)
29. Pineda, M., Toral, R., Hernández-García, E.: The noisy Hegselmann-Krause model for opinion dynamics. Eur. Phys. J. B **86**(12), 1–10 (2013)
30. Touri, B., Nedić, A.: Discrete-time opinion dynamics. In 2011 Conference Record of the Forty-Fifth Asilomar Conference on Signals, Systems and Computers (ASILOMAR) (2011)
31. Wedin, E., Hegarty, P.: A quadratic lower bound for the convergence rate in the one-dimensional Hegselmann-Krause bounded confidence dynamics. Discret. Comput. Geom. **53**(2), 478–486 (2015)